Electronic Supporting Information

Stabilization of Volatile $Ti(BH_4)_3$ by nano-confinement in a Metal-Organic Framework

Elsa Callini[*]*, Petra Á. Szilágyi, Mark Paskevicius, Nicholas P. Stadie, Julien Réhault, Craig E. Buckley, Andreas Borgschulte and Andreas Züttel*

Supplementary Figure S1

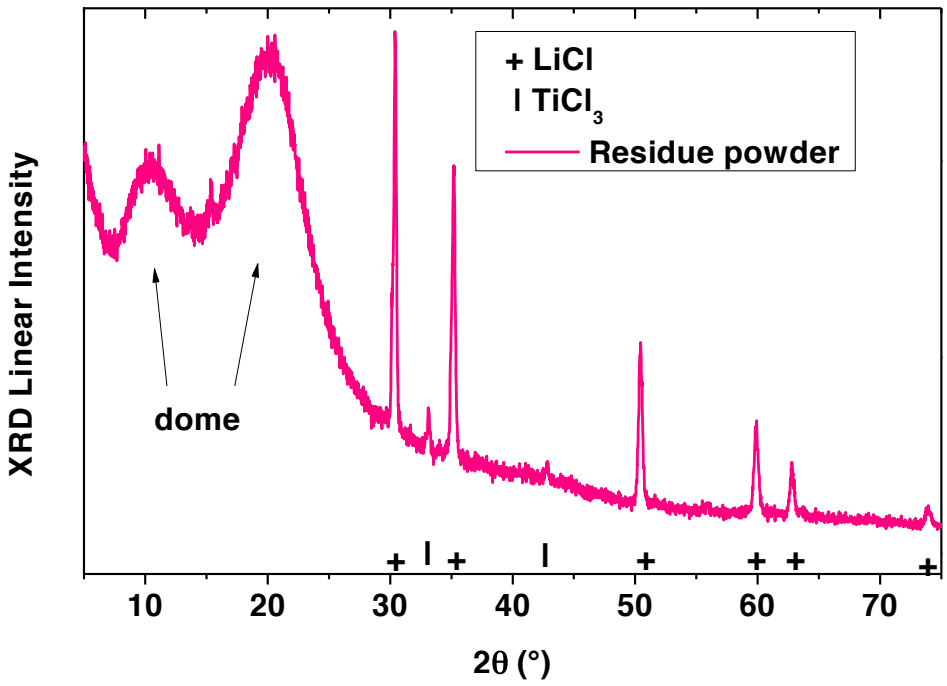

XRD at room temperature on the residue powder after metathesis and $Ti(BH_4)_3$ evaporation. The main crystalline phase is LiCl, showing that the metathesis successfully occurred. The humps at roughly 10 and 20° are due to the PMMA dome.

Supplementary Figure S2

Pictures showing the white pristine MOF before adsorption (left) and the grey grains of the MOF after $Ti(BH_4)_3$ adsorption (right) in the glove box.

Supplementary Figure S3

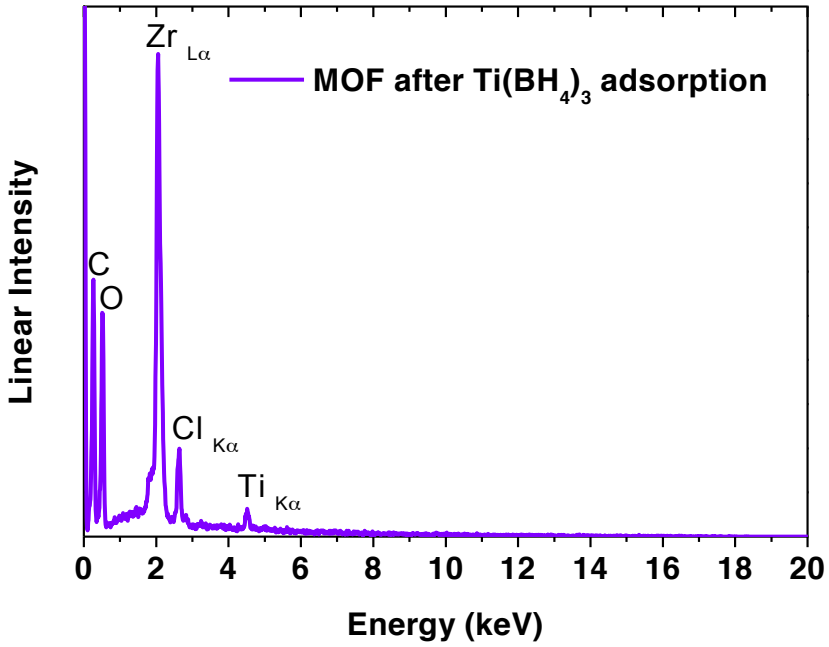

EDX on the impregnated MOF, showing a discernible Ti signal due to $Ti(BH_4)_3$ adsorption. Zr, C and O are in the MOF itself; Cl is a residue from the MOF preparation.

Supplementary Figure S4

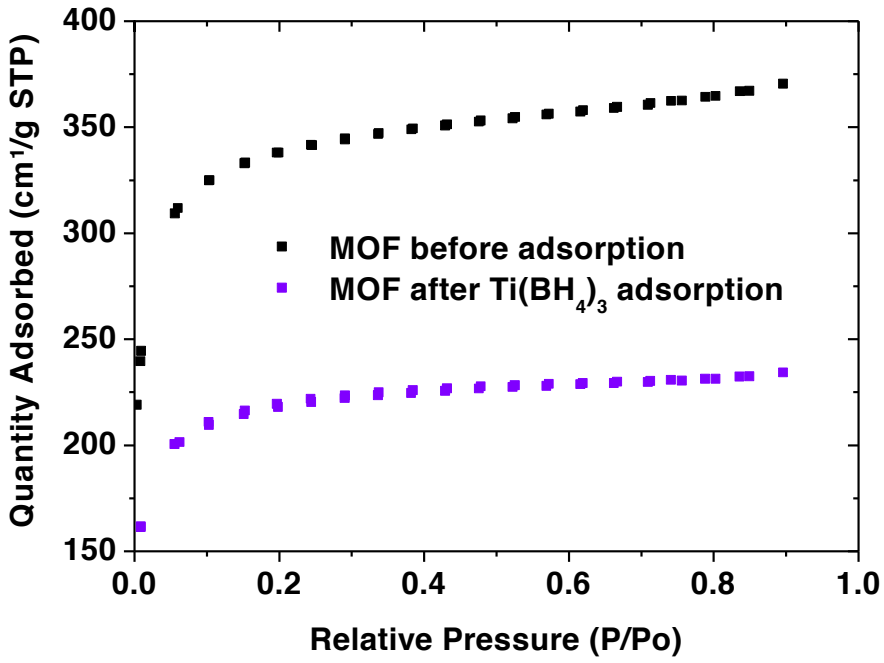

Equilibrium N_2 adsorption isotherms at 77 K on the pristine (black) and loaded (purple) MOF. The BET Surface Area is decreased by a factor 2 in the loaded MOF: BET surface area of the pristine MOF is approximately 1200 m^2/g, while the BET surface area of the loaded MOF is approximately 770 m^2/g.

Supplementary Figure S5

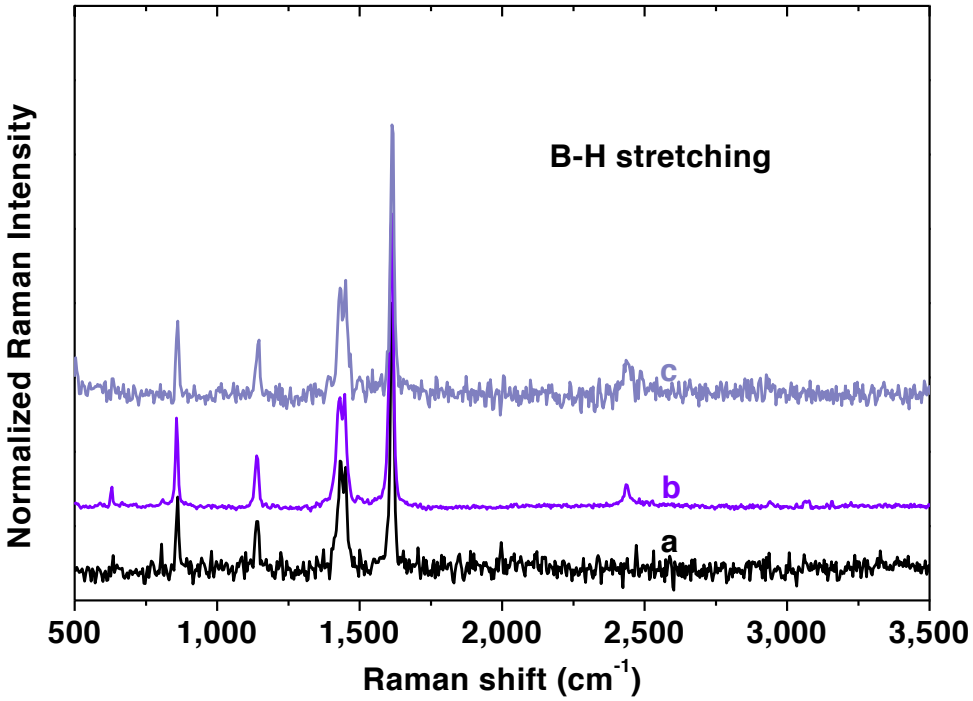

Raman spectra showing the successful gas adsorption on the MOF and the stabilisation of the gas molecule.

Raman spectra at room temperature of (a) the pristine MOF, (b) the impregnated MOF and (c) the impregnated MOF after 1 month in argon atmosphere, ambient pressure and room temperature. The vibrations are assigned as follows: 630 cm^{-1} Zr-O stretching; 650-900 cm^{-1} C-H out of plane bending; 1140 cm^{-1} C-H in plane bending; 1430-1625 cm^{-1} C-C stretching as in Ref. 40 in the main text; 2435 cm^{-1} B-H stretching, visible only in the loaded sample. The guest molecules may interact with either the cationic node or the linker, but the MOF peaks are not altered by the gas adsorption. Zr-O bonds are very strong and unlikely to change significantly. In addition to that, the total number of building blocks in the host is much greater than that of the guest molecules and in case of interaction we would only anticipate small peaks shifts: due to the instrumental spectral resolution, a Raman shift smaller than ±3 cm^{-1} would not be resolved.

The data were fitted with Lorentzian functions (see main text), whose centres and widths are listed below. All the fits did not take into account the mode at 630cm^{-1} and converged to a R^2 > 0.97. The error for the centre determination was estimated as ± 3 cm^{-1}. The fit of the spectrum of the unloaded MOF did not converge when 6 Lorentzian peaks were selected. As expected, the fit converged with 5 Lorentzian functions, listed below with numbers 1 - 5.

Peaks

Number	Centre
1	859
2	1140
3	1428
4	1447
5	1612
6	2437

Supplementary Figure S6

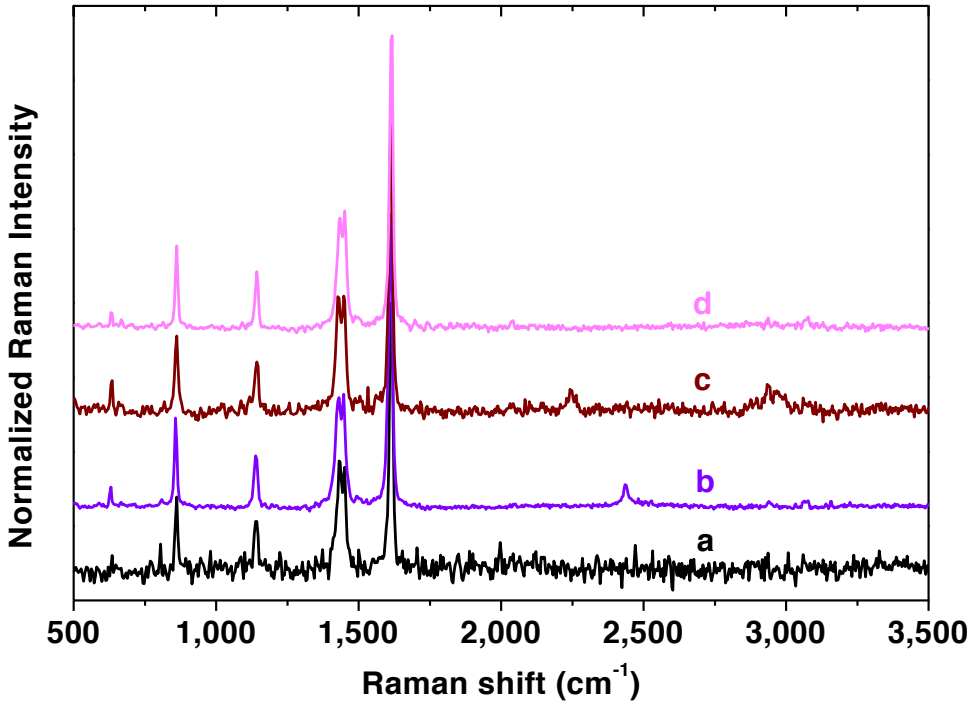

Raman spectra showing the decomposition of the loaded MOF.

Raman spectra at room temperature of (a) the pristine MOF, (b) the loaded MOF, (c) the loaded MOF after temperature ramp in vacuum up to 470 K and (d) the loaded MOF after TPD-MS and air exposure. The vibrations are assigned as follows: 630 cm^{-1} Zr-O stretching; 650-900 cm^{-1} C-H out of plane bending; 1140 cm^{-1} C-H in plane bending; 1430-1625 cm^{-1} C-C stretching, as in Ref. 40 in the main text; 2435 cm^{-1} B-H stretching, visible only in the loaded sample before heat treatment; 2245 and 2950 cm^{-1} B-H stretching, visible only in the sample after heat treatment.

The data were fitted with Lorentzian functions (see main text), whose centres and widths are listed below. All the fits did not take into account the mode at 630cm^{-1} and converged to a R^2 > 0.97. The error for the centre determination was estimated as ± 3 cm^{-1}. The fit for the spectrum of the unloaded MOF converged with 5 Lorentzian functions, listed below with numbers 1 - 5. The fit for the spectrum of the loaded MOF converged with 6 Lorentzian functions, listed below with numbers 1 - 5 and 7. The fit for the spectrum of the loaded MOF

after temperature ramp in vacuum up to 470 K converged with 7 Lorentzian functions, listed below with numbers 1 - 6 and 8. The fit for the spectrum of the loaded MOF after TPD-MS and air exposure converged with 6 Lorentzian functions, listed below with numbers 1 - 5 and 8. For this latter fit, the B-H peak at roughly 2940 cm^{-1} is barely visible in spectrum d (intensity 0.4% with respect to spectrum c), showing just a residue of the decomposition of the species.

Peaks

Number	Centre
1	862
2	1142
3	1428
4	1447
5	1613
6	2246
7	2437
8	2940

Supplementary Figure S7

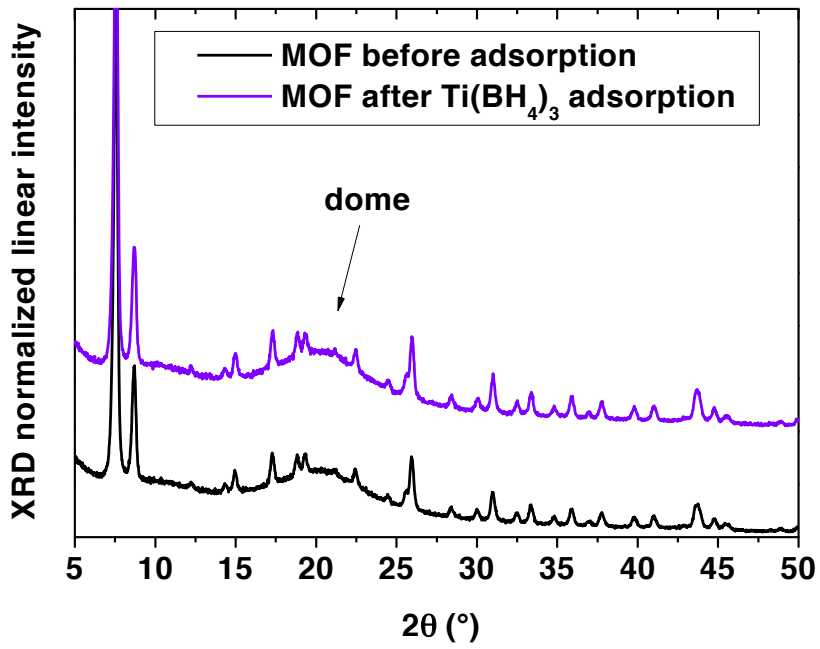

XRD at room temperature on the MOF before and after $Ti(BH_4)_3$ adsorption. The peaks can all be assigned to the UiO-66 MOF as in Ref. 25 in the main text. The hump at roughly 20° is due to the PMMA dome. The two patterns are almost identical, showing that there was no significant reaction between the MOF and the gas molecules.

Supplementary Table S1

MOF	Pore Diameter Adsorption (Å)	Pore Diameter Desorption (Å)
UiO-66	26.62 ± 0.21	26.54 ± 0.21
$Ti(BH_4)_3$⊂UiO-66	23.18 ± 0.21	21.61 ± 0.21
Change	3.44 ± 0.30	4.93 ± 0.30

Barrett-Joyner-Halenda (BJH) pore-size analysis.

The analysis estimates the average size of the pores, assuming that the pores have a cylindrical shape as in Ref. 38 in the main text. We observed a decrease of the average pore width in the loaded MOF of 3.44 Å with respect to the pore width of pure MOF (adsorption). $Ti(BH_4)_3$ molecules can be approximated as cylinders, whose diameter is roughly 7 Å and the length is 2 Å. It is therefore suggested that on average there is more than one $Ti(BH_4)_3$ molecule per UiO-66 pore.